A comparison of hydrogen storage capacity of commercial and fly ash-derived zeolite X together with their respective templated carbon derivatives

Nicholas M. Musyoka*

NMusyoka@csir.co.za

Jianwei Ren

Henrietta W. Langmi

Brian C. North

Mkhulu Mathe

HySA Infrastructure Centre of Competence, Materials Science and Manufacturing, Council for Scientific and Industrial Research (CSIR), South Africa

*Corresponding author.

Abstract

This paper presents comparative results of structural, morphological and hydrogen sorption properties between commercial and fly ash-derived zeolite X including their respective templated carbon derivatives. The surface area of commercial zeolite was found to increase by 328% from 796 $m^2 g^{-1}$ to 2578 $m^2 g^{-1}$ upon templation process whereas that of fly ash-derived zeolite increased by 275% from 404 $m^2 g^{-1}$ to 1112 $m^2 g^{-1}$ on templation. The trend in hydrogen uptake was also proportionally mirrored by the surface area. Commercial analysis estimated that the cost of synthesizing zeolite X from fly ash is one fifth that of the existing commercial zeolite production process. The use of fly ash-derived zeolites is expected to present a cost effective and competitive way of producing zeolite templated carbons. Additionally, fly ash zeolitization together with its use in the synthesis of templated carbons also present an attractive way of beneficiating coal fly ash.

Keywords: Zeolite X; Templated carbon; Fly ash; Hydrogen storage

Introduction

The search for environmentally friendly alternative energy sources has led to intensification of research amongst others on applications of hydrogen as an alternative energy carrier [1,2]. The main advantages of the use of hydrogen energy over the other energy sources are mainly due to its zero green-house gas emissions during use, high energy density properties plus its potential to be derived from electrolysis of water [3,4]. The major bottleneck inhibiting the widespread adoption of hydrogen energy is deemed to be lack of safe, reliable and recyclable methods of hydrogen storage [2,5,6]. In order to address these challenges, many researchers have intensified their research in hydrogen storage technologies [2,7,8]. The main hydrogen storage technologies are based on liquefied, compressed or materials-based hydrogen storage options [7]. Since materials-based storage option is reported to be promising [8–10], numerous studies have specifically concentrated on applications of porous materials in hydrogen storage [4–6]. Among the many studied porous materials (such as zeolites, metal organic frameworks (MOFs), activated carbons etc.), templated carbons have been identified and ear-marked as having attractive properties for hydrogen storage [11–15]. Templated carbons are typically of microporous or mesoporous carbonaceous materials synthesised by impregnation of a carbon precursor into the pores or micro/meso-channels of an inorganic template [2,12]. Among the many templates that have been investigated [11,13], zeolites are reported to lead to preparation of well-structured micro-porous/meso-porous carbons with high surface areas, large micro-pore volumes and exhibit impressive hydrogen adsorption properties [11,14]. The main challenge likely to inhibit scale-up production of zeolite-templated carbons has recently been identified as the potentially high cost of production [13]. Therefore, there is a need to explore the possibility for the use of zeolite templates produced from cheap unconventional synthesis feedstocks [15]. An estimated synthesis cost of zeolite X from fly ash is one fifth that of the producing commercial zeolite X [16], thus the use of fly ash-derived zeolite X presents a cost effective and competitive way of producing templated carbons. Additionally, fly ash zeolitization also present an attractive environmentally friendly way of beneficiating coal fly ash. Our current study therefore aims at demonstrating/showing that fly ash-derived zeolites would potentially act as a cheaper and alternative feedstock for producing the much sought-after templated carbons.

Materials and procedure for sample preparation

Commercially available zeolite X (Sigma Aldrich) and fly ash-derived zeolite X were used as the templating agents. The fly ash-derived zeolite X preparation procedure is reported previously in Ref. [17]. The as-synthesized zeolite was further ion-exchanged to flush out any remaining transition metal elements (e.g. Fe, Ni, Co, Mo, etc) that could potentially act as a catalyst for the growth of carbon nanotubes during the templation process [15]. The ion-exchange procedure was

as follows: the as-synthesized fly ash-derived zeolite was mixed with ammonium nitrate (1 M) and gently stirred for 12 h. The resulting samples were vacuum filtered and washed with deionized water. The ion-exchange procedure was repeated 3 times and thereafter the samples were dried at 90 °C for 12 h. To burn off the NH_4^+ ion in the sample, the ion exchanged samples were calcined at 500 °C for 4 h in the tube furnace under the flow of Argon. Furfuryl alcohol (Sigma Aldrich, $C_5H_6O_2$, 98%) and Ethylene gas (99.99%) were used as the carbon precursors. Ethanol (Merck, 99.5%) was used as solvent. Hydrofluoric (Merck, 40%) and hydrochloric acids (Ace, 32%) were used to remove the inorganic template from the resulting carbon. The procedure for preparation of the zeolite templated carbons is as reported in our previous work [15].

Characterization

Powder X-ray diffraction (XRD) patterns were acquired using a PANalytical X'Pert Pro powder diffractometer, fitted with a Pixcel detector and with Cu-Kα radiation (0.154 nm). The diffractograms were collected within the range of $2\theta = 4$–$60°$. Morphological analysis was performed using a scanning electron microscope (Jeol-JSM 7500F). The samples were mounted on a copper stub laced with a conductive sticky carbon tape and carbon coated to avoid charging during analysis. Transmission electron microscope (TEM) images were recorded using a JEOL-Jem 2100 model. The samples for TEM measurements were sonicated in ethanol and drop-dried onto a holey carbon film supported on a copper grid. Thermal stability analysis was performed using a thermo-gravimetric analysis (TGA) instrument (Mettler, Toledo, TGA/SDTA 851e). In this case, about 10 mg of the sample was loaded in an alumina crucible and heated to 1000 °C at a rate of 10 °C min^{-1} with an air flow of 10 mL min^{-1}. Nitrogen sorption measurement (surface area and porosity) were performed using an ASAP 2020 HD analyzer (Micromeritics). The samples were out-gassed prior to analysis under vacuum at 350 °C for 8 h. BET surface areas were obtained from the linear region of the N_2 isotherms. Micro-pore volumes were calculated from the Dubinin–Radushkevich (DR) equation using the adsorption isotherms data. Pore size distributions (PSDs) plots were obtained using non-local density functional theory (DFT). Hydrogen adsorption isotherms, at 77 K and up to 1 bar, were also measured on the ASAP 2020 instrument. All gas sorption isotherms were obtained using ultra-high purity grade (99.999%) gas. Before analysis, the samples were outgassed for 8 h at 350 °C in the degassing port with further degassing at 300 °C for 3 h in the analytical port.

Results and discussion

Fig. 1a–c shows the XRD patterns, SEM images and TEM images of commercial zeolite X together with its templated carbon derivative. The XRD diffraction pattern of commercial zeolite (Fig. 1a) shows the expected diffraction peaks associated with zeolite X whereas its templated carbon derivative exhibited a dominant peak at around $2\theta = 7°$, indicative of regular ordering with periodicity of about 1.4 nm in the carbon structure [14,18]. It was also noted that the many peaks associated with the parent zeolite were absent in the carbonaceous material. SEM images (Fig. 1b) reveals the octahedral-pyramidal morphology that is typically associated with zeolite X and also shows that the resulting templated carbonaceous material had similar morphological features as that of the parent zeolitic material. The high-resolution TEM image (Fig. 1c) shows zeolite-like fringes with periodicity that confirms structure regularity. The aligned fringes corresponded to the (111) plane of zeolite as was shown by the XRD peak appearing at about $2\theta = 7°$ in Fig. 1a. The diffuse halo shown by the selected area diffraction pattern (SAED) is indicative of scattering from an amorphous material meaning that, unlike the parent zeolite, the templated carbon derivative was amorphous in nature.
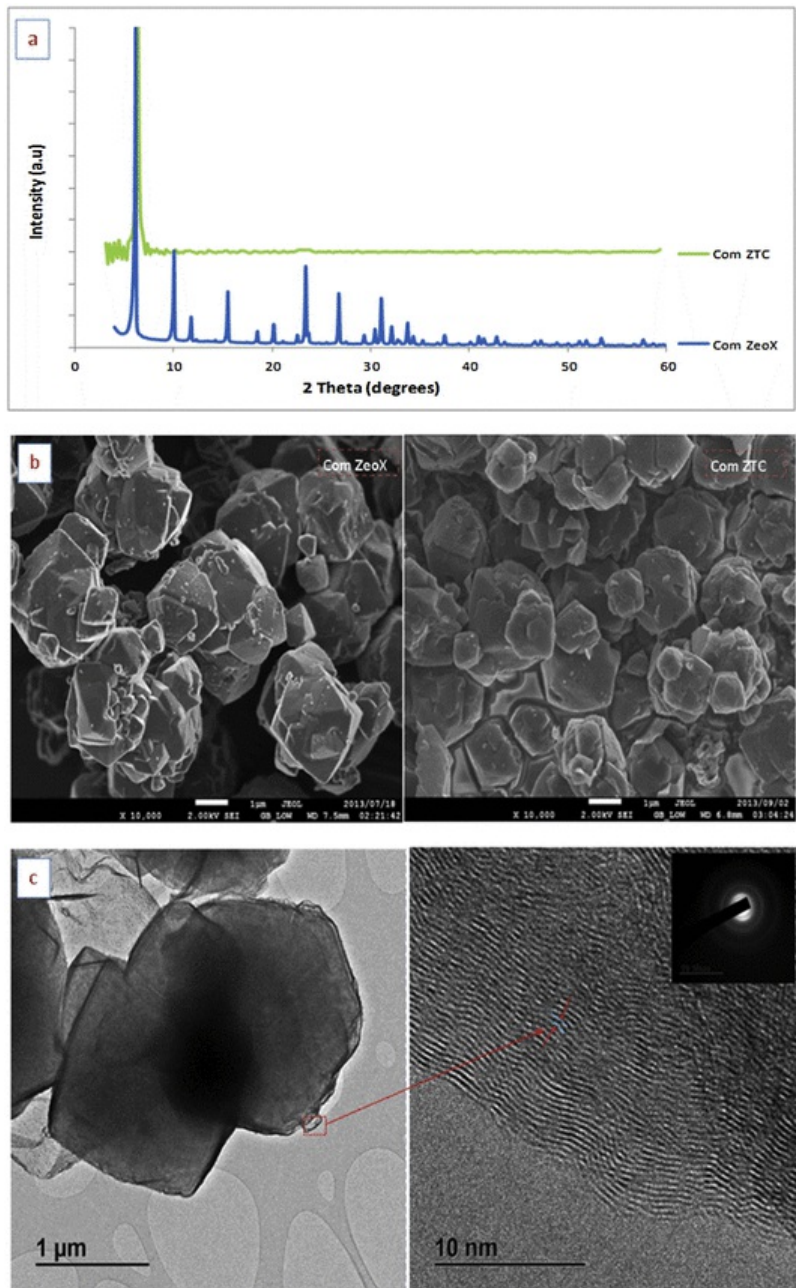
Fig. 1 (a) XRD patterns and (b) SEM images of commercial zeolite (Com ZeoX) together with its templated carbon derivative (Com ZTC), c) TEM images (low and high resolution) of templated carbon derivative (Com ZTC).

Comparing the XRD pattern of fly ash-derived zeolite X (Fig. 2a) with that of its commercial counterpart (Fig. 1a), it is evident that their diffraction patterns were similar. On the other hand, their templated carbon derivative were different since the fly ash zeolite templated carbon had a broad XRD peak observed at $2\theta = 26°$ and at around $45°$ which was suggestive of the presence of disorderly oriented tiny graphenic type fragments in the structures [1]. The diffraction peak at

around 2θ = 26° can be ascribed to correspond to the (002) diffraction of graphitic carbon [19]. Unlike activated carbons [2], these zeolite templated carbons were observed to show evidence of microstructural ordering through the appearance of Bragg peaks in their XRD patterns. Early studies by Mokaya's group [20,21] reported that formation of large amounts of graphitic carbon is mainly due to the deposition of carbon outside the pores of the zeolite template. This eternally deposited carbon has been reported to grow without any spatial restriction, which either causes obstruction of access to the zeolite pores or even accelerates the carbonisation of the carbon precursor once it comes in contact with the zeolite [18]. The SEM images of fly ash-derived zeolite X together with its templated carbon derivative (Fig. 2b) show that the morphology of the parent zeolite was also realistically replicated in the templated carbon. The particle size of the templated carbon from fly ash-derived zeolite was significantly reduced due to the effects of ion-exchange that was conducted prior to the templating process.
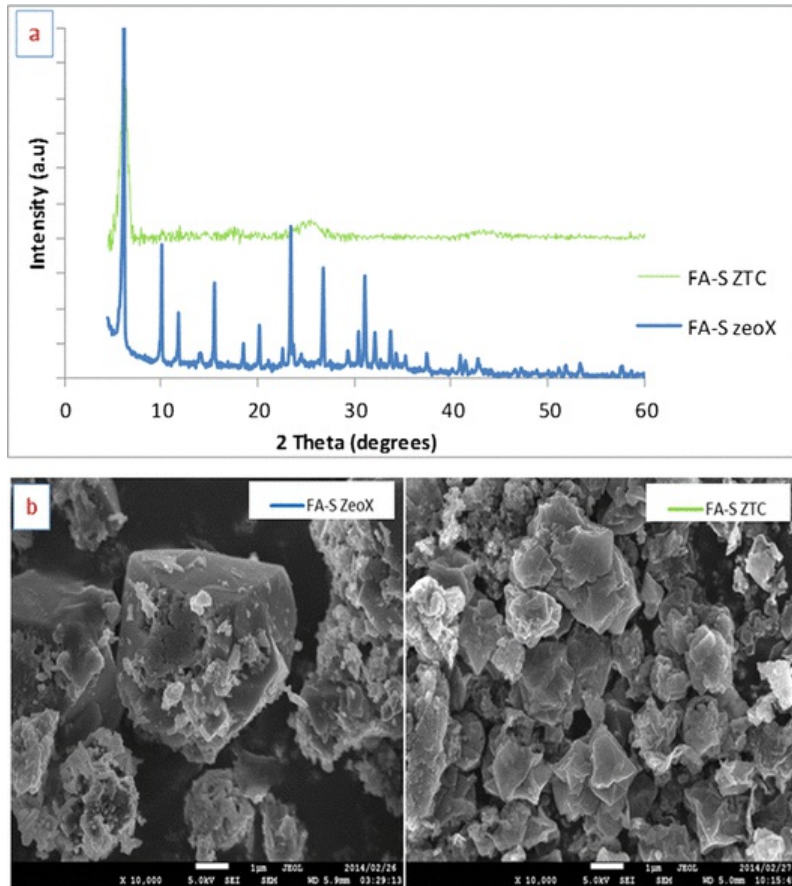

Fig. 2 XRD patterns (a) and SEM images (b) of fly ash-derived zeolite (FA-S ZeoX) together with its templated carbon derivative (FA-S ZTC).

The TGA plots in Fig. 3 confirm that both template synthesis products from the commercial and fly ash-derived zeolite were mainly composed of carbon (~99%) which implied that the template removal process was done successfully.
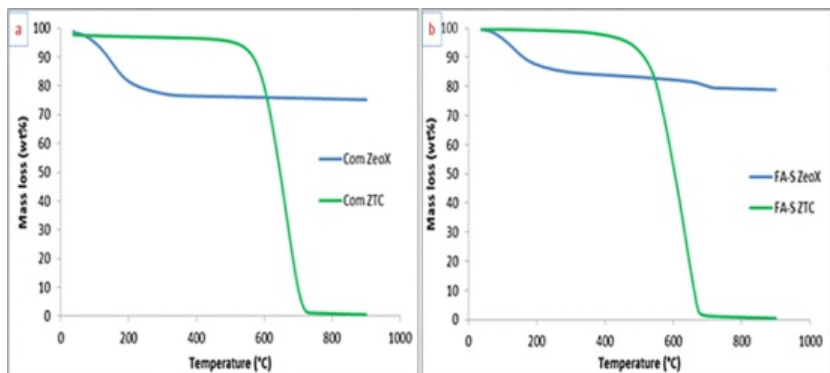
Fig. 3 A comparison of TGA plots of: (a) commercial zeolite X (Com ZeoX) and (b) fly ash-derived zeolite X (FA-S ZeoX) together with their respective zeolite templated carbons (Com ZTC and FA-S ZTC).

Fig. 4 shows that the nitrogen adsorption isotherms, at 77 K, for both commercial and fly ash derived zeolites were mainly of Type I nature which is indicative of a microporous structure [22]. The limiting factor in the quantity of gas adsorbed in this type of materials is reportedly governed by the accessible micropore volume rather than by the internal surface area [23]. The steep adsorption at a $P/P_0 < 0.03$ suggests presence of a significant amount of micropores with a narrow pore size distribution. Upon templation, the isotherm of the templated carbon from commercial zeolite also exhibited the Type I nature with a negligible hysteresis. The presence of micropores in this nano-casted carbon is consistent with the zeolite-like structural ordering observed in Fig. 1c. On the other hand, the nitrogen sorption isotherms of templated carbon from fly ash-derived zeolite exhibited relatively lower adsorption at $P/P_0 < 0.03$ but showed inexplicably much higher adsorption at $P/P_0 > 0.9$. The hysteresis loop which is associated with capillary condensation taking place in mesopores was also observed to be much wider in fly ash-derived zeolite templated carbon than that of the commercial zeolite derivative. The presence of the hysteresis would make the isotherm to be classified as Type IV [23]. As explained above, incomplete infiltration of the carbon precursor into the zeolite micro-channels [19] is thought to have led to formation of mesopores when the zeolitic template was removed.
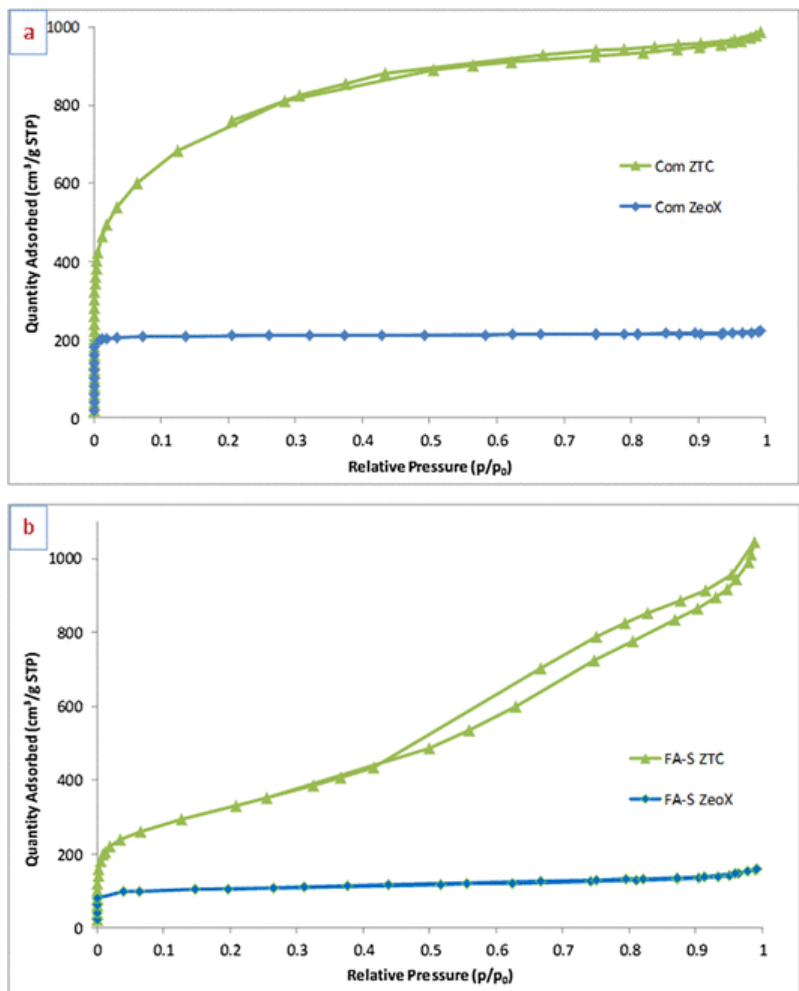
Fig. 4 A comparison of BET isotherm plots of: (a) commercial zeolite X (Com ZeoX) and (b) fly ash derived zeolite X (FA-S ZeoX) together with their respective zeolite templated carbons (Com ZTC and FA-S ZTC).

Table 1 summarizes the textural parameters and hydrogen uptake capacities of commercial zeolite X and fly ash derived zeolite X together with their respective zeolite templated carbons. The surface area of commercial zeolite was found to increase from 795.5 $m^2 g^{-1}$ to 2577.8 $m^2 g^{-1}$ upon templation process whereas that of fly ash-derived zeolite increased from 404.1 $m^2 g^{-1}$ to 1112.2 $m^2 g^{-1}$ on templation. This improvement in surface area was also relative to the increased micropore volumes. The hydrogen uptake capacity of templated carbon from fly ash-derived zeolite of 1.2 wt% was found to be half that obtained from commercial zeolite which is 2.4 wt%. The difference can be explained by the variations in their respective pore size distributions.

Table 1 Physical properties and H_2 uptake capacities of commercial zeolite X and fly ash derived zeolite X together with their respective zeolite templated carbons.

Sample	BET specific surface area ($m^2 g^{-1}$)	Micropore volume ($cm^3 g^{-1}$)	H_2 uptake, 77 K and 1 bar (wt%)
Com zeoX	795.5	0.35	1.6
FA-S zeoX	404.1	0.17	0.7
Com ZTC	2577.8	1.44	2.4

| FA-S ZTC | 1112.2 | 0.48 | 1.2 |

The pore size distribution of templated carbon derived from commercial zeolite was found to be between 1 and 2 nm whereas the fly-ash derived zeolite templated carbons had most pores appearing between 2 and 7 nm (Fig. 5). Furthermore, the pore size distribution of templated carbon from commercial zeolite was found to be quite narrow compared to that from fly ash derived zeolite. The reason for the pore size distribution difference could be attributed to the potential differences in the Si/Al of the zeolites. Studies of the effect of Al content on the properties and hydrogen storage capacity of resulting zeolite templated carbons in Ref. [18] have highlighted that differences in the Al content in zeolite could have the potential of accelerating the rate of carbonisation. The initial formation of carbon on the surface of the zeolite could potentially cause blockage of carbon precursors from infiltrating the interior nanospace of the zeolites template. When the template is removed from the regions that had poor ingress of the carbon precursor there is a higher chance for formation of the mesoporosity, as observed in this case. The differences in pore size distribution have also been reported to influence the hydrogen uptake capacities [13,19]. Moreover, the presence of a large number of ultramicropores is known to lead to higher isosteric heat of adsorption and hence a stronger interaction between carbon and hydrogen [18].
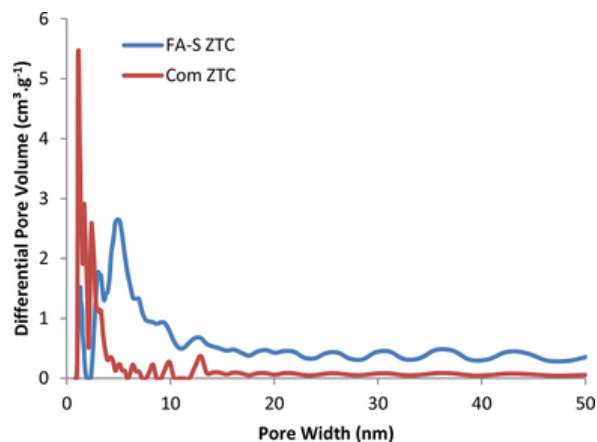

Fig. 5 Pore size distributions (PSDs) of zeolite templated carbons from commercial zeolite (Com ZTC) and fly ash-derived zeolite (FA-S ZTC).

The hydrogen uptake isotherms of the all the zeolites (Com ZeoX, FA-S ZeoX) and their respective templated carbons, at 77 K over the pressure range 0–1 bar, are shown in Fig. 6. As reported by other researchers [18], the hydrogen uptake isotherms were evaluated on the basis of a density of 1.5 g cm^{-3} for the templated carbon samples. The hydrogen uptake capacities are summarised in Table 1 and the relationship between surface area and hydrogen uptake of all the templated carbons is well established. From Fig. 6, it can be noted that the hydrogen storage capacity in zeolite-templated carbon was relatively higher when compared to that of the parent zeolitic material. This observation is supported by other previous studies [24–26] that have established a correlation between hydrogen uptake and surface area of porous materials.
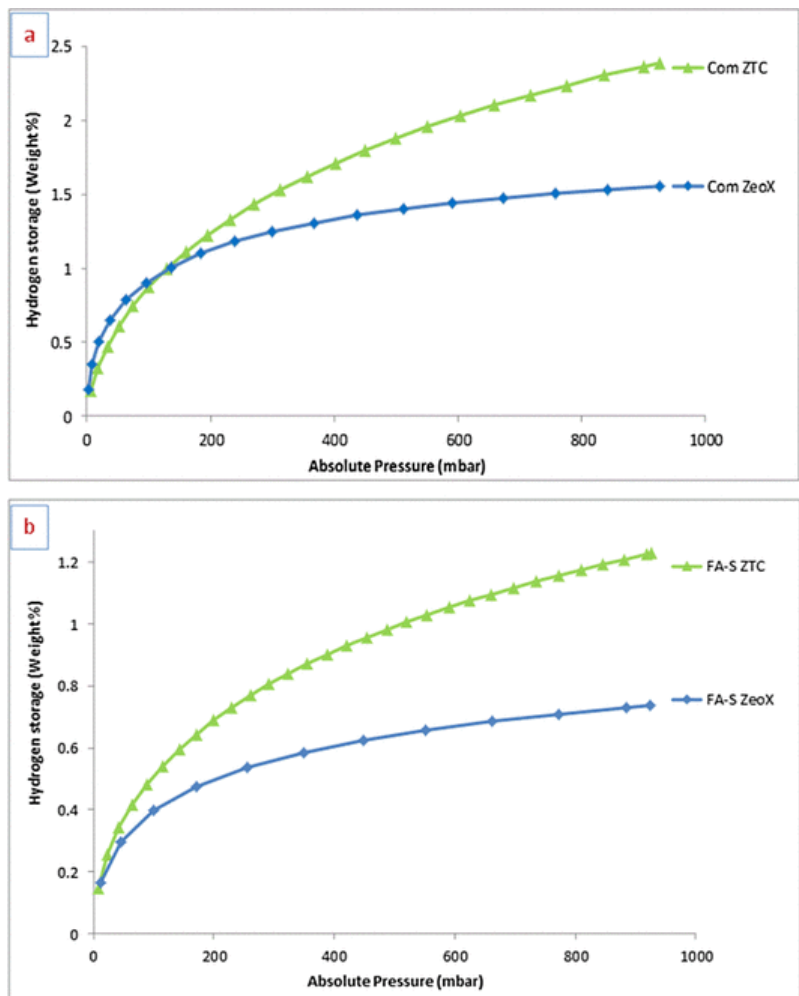
Fig. 6 A comparison of: (a) hydrogen uptake isotherms of commercial zeolite X (Com ZeoX) and (b) fly ash derived zeolite X (FA-S ZeoX) together with their respective zeolite templated carbons (Com ZTC and FA-S ZTC).

As would be expected, the trend in surface area (Table 1) was proportionally mirrored by the hydrogen uptake isotherms (Fig. 6) in which case high surface area and a large micro-pore volume of the templated carbon from commercial zeolite lead to the highest hydrogen storage capacity of 2.2 wt%. The isotherms of the zeolite templated carbons shown in Fig. 6 also clearly indicate that saturation was not attained at 1 bar and thus higher hydrogen uptake capacities are expected at pressure exceeding 1 bar. Even though the hydrogen storage capacity of carbon from fly ash-derived zeolite was not equivalent to that obtained from the commercial zeolite, careful selection of the synthesis procedure and/or post synthesis modifications would be expected to generate better properties that could potentially lead to improvements in the hydrogen uptake capacities.

Conclusion

Synthesis of zeolite templated carbons starting from both commercial and fly ash-derived zeolite X was successfully accomplished. The BET surface areas and micropore pore volumes of templated carbons were found to be significantly higher than that of the zeolite template, which also lead to enhanced hydrogen storage capacity. It was found that the proportion of micropores (<2 nm) to that mesopores (>2 nm) was relatively lower in fly ash based carbon when compared to those of carbon from commercial zeolite. The use of fly ash-derived derived zeolites, as unconventional templating agent, has the potential of providing a cost effective alternative for producing templated carbonaceous materials for hydrogen storage applications. The present study was not aimed to optimise the hydrogen storage capacity of fly ash-derived zeolite templated carbons. Further follow up studies still need to be conducted to improve the quality of the fly ash

zeolite for improved hydrogen storage capacity so that the resulting properties are comparable with those of the commercial counterpart.

Acknowledgements

References

[1]

Y. Yang, L. Bourgeois, C. Zhao, D. Zhao, A. Chaffee and P.A. Webley, Ordered micro-porous carbon molecular sieves containing well-dispersed platinum nanoparticles for hydrogen storage, *Microporous Mesoporous Mater* **119**, 2009, 39–46.

[2]

D.P. Broom, Hydrogen storage materials: the characterisation of their storage properties, Series: Green Energy and Technology2011, Springer; London.

[3]

R. Ramachandran and R.K. Menon, An overview of industrial uses of hydrogen, *Int J Hydrogen Energy* **23**, 1998, 593–598.

[4]

J.A. Alonso, I. Cabria and M.J. López, The storage of hydrogen in nanoporous carbons, *J Mex Chem Soc* **56**, 2012, 261–269.

[5]

B. Panella, M. Hirscher and S. Roth, Hydrogen adsorption in different carbon nanostructures, *Carbon* **43**, 2005, 2209–2214.

[6]

A.M. Ruminski, R. Bardhan, A. Brand and J.J. Urban, Future prospects for hydrogen storage in designer nanocomposites, *Biofuels* **2**, 2011, 591–594.

[7]

D.J. Durbin and C. Malardier-Jugroot, Review of hydrogen storage techniques for on board vehicle applications, *Int J Hydrogen Energy* **38**, 2013, 14595–14617.

[8]

A.W.C. Van den berg and C.O. Areán, Materials for hydrogen storage: current research trends and perspectives, *Chem Commun* 2008, 668–681.

[9]

S. McWhorter, C. Read, G. Ordaz and N. Stetson, Materials-based hydrogen storage: attributes for near-term, early market PEM fuel cells, *Curr Opin Solid St Mater* **15**, 2011, 29–38.

[10]

K.L. Lim, H. Kazemian, Z. Yaakob and W.R.W. Daud, Solid-state materials and methods for hydrogen storage: a critical review, *Chem Eng Tech* **33**, 2010, 213–226.

[11]

Y. Xia, Z. Yang and Y. Zhu, Porous carbon-based materials for hydrogen storage: advancement and challenges, *J Mater Chem A* **1**, 2013, 9365–9381.

[12]

X.H. Song, R. Xu and K. Wang, The structural development of zeolite-templated carbon under pyrolysis, *J Anal Appl Pyrol* **100**, 2013, 153–157.

[13]

H. Nishihara and T. Kyotani, Templated nanocarbons for energy storage, *Adv Mater* **24**, 2012, 4473–4498.

[14]

E. Masika and R. Mokaya, Preparation of ultrahigh surface area porous carbons templated using zeolite 13X for enhanced hydrogen storage, *Prog Natl Sci* **23**, 2013, 308–316.

[15]

N.M. Musyoka, J.W. Ren, H.W. Langmi, D.E.C. Rogers, B.C. North, M. Mathe, et al., Synthesis of templated carbons starting from clay and clay-derived zeolites for hydrogen storage applications, *Int J Energy Res* **39**, 2015, 494–503.

[16]

K. Ojha, N.C. Pradhan and A.N. Samanta, Zeolite from fly ash: synthesis and characterization, *Bull Mater Sci* **27**, 2004, 555–564.

[17]

N.M. Musyoka, L.F. Petrik, O.O. Fatoba and E. Hums, Synthesis of zeolites from coal fly ash using mine waters, *Min Eng* **53**, 2013, 9–15.

[18]

N. Alam and R. Mokaya, The effect of Al content of zeolite template on the properties and hydrogen storage capacity of zeolite templated carbons, *Microporous Mesoporous Mater* **144**, 2011, 140–147.

[19]

S. Lee and S. Park, Synthesis of zeolite-casted microporous carbons and their hydrogen storage capacity, *J Colloid Interface Sci* **384**, 2012, 116–120.

[20]

Z. Yang, Y. Xia and R. Mokaya, Enhanced hydrogen storage capacity of high surface area zeolite-like carbon materials, *J Am Chem Soc* **129**, 2007, 1673–1679.

[21]

A. Pacuła and R. Mokaya, Synthesis and high hydrogen storage capacity of zeolite-like carbons nanocast using as-synthesized zeolite templates, *J Phys Chem C* **112**, 2008, 2764–2769.

[22]

K.S.W. Sing, D.H. Everett, R.A.W. Haul, L. Moscou, R.A. Pierottl, J. Rouquerol, et al., Reporting physisorption data for gas/solid systems with special reference to the determination of surface area and porosity (Recommendations 1984), *Pure Appl Chem* **57**, 1985, 603–619.

[23]

S. Lowell, J.E. Shields and M.A. Thomas, Characterization of porous solids and powders: surface area, pore size and density, 2006, Springer. ISBN: 1402023022.

[24]

R. Chahine and T.K. Bose, Low-pressure adsorption storage of hydrogen, *Int J Hydrogen Energy* **19**, 1994, 161–164.
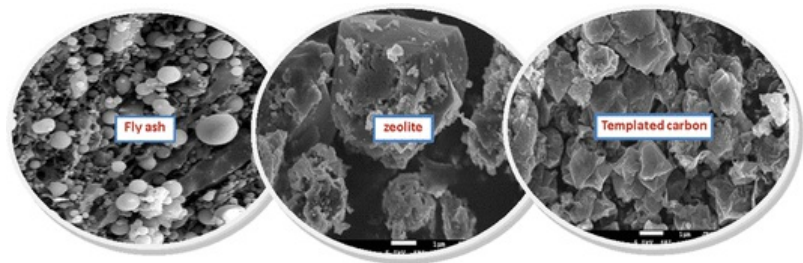
[25]

R. Chahine and T.K. Bose, Characterization and optimization of adsorbents for hydrogen storage. hydrogen energy progress XI, *Proc 11th World Hydrogen Energy Conf* **2**, 1996, 1259–1263.

[26]

B. Panella, M. Hirscher, H. Putter and U. Muller, Hydrogen adsorption in metal-organic frameworks: Cu-MOFs and Zn-MOFs compared, *Adv Funct Mater* **16**, 2006, 520–524.

Graphical abstract

Highlights

- The study compared the use of commercial and fly ash-derived zeolites as templated for synthesis of carbons.

- Templated carbons had a higher hydrogen uptake than their parent zeolites.

- The use of fly ash-derived zeolites presents a cost effective and competitive way of producing templated carbons.

Queries and Answers

Query: Please provide the grant number for 'South African Department of Science and Technology (DST)' if any.

Answer: The information is provided as; 'South African Department of Science and Technology (DST) for the HySA programme (Project No.: HTC004X).'

Query: Please confirm that given names and surnames have been identified correctly.

Answer: The names are correctly identified.

Query: Your article is registered as a regular item and is being processed for inclusion in a regular issue of the journal. If this is NOT correct and your article belongs to a Special Issue/Collection please contact a.mutale1@elsevier.com immediately prior to returning your corrections.

Answer: The current article is regular issue of the journal.